This manuscript was published as

Heckel, B., Phillips, E., Edwards, E., Sherwood Lollar, B., Elsner, M., Manefield, M.J., Lee, M.: Reductive dehalogenation of trichloromethane by two different dehalobacter restrictus strains reveal opposing dual element isotope effects. Environ. Sci. Technol. 53, 2332-2343 (2019), doi: 10.1021/acs.est.8b03717

Reductive dehalogenation of trichloromethane by two different *Dehalobacter restrictus* strains reveal opposing dual element isotope effects

Benjamin Heckel[a,b*], *Elizabeth Phillips*[c], *Elizabeth Edwards*[d], *Barbara Sherwood Lollar*[c], *Martin Elsner*[a,b], *Mike Manefield*[e], *Matthew Lee*[e*]

[a]Institute of Groundwater Ecology, Helmholtz Zentrum München, Ingolstädter Landstr. 1, 85764 Neuherberg, Germany

[b]Chair of Analytical Chemistry and Water Chemistry, Technical University of Munich, Marchioninistrasse 17, D-81377 Munich, Germany

[c]Department of Earth Sciences 22 Russell St, University of Toronto, Toronto Ontario, M5S 3B1, Canada

[d]Department of Chemical Engineering and Applied Chemistry, University of Toronto, Toronto, ON M5S 3E5, Canada

[e]School of Civil and Environmental Engineering's Water Research Centre (WRC), University of New South Wales, Sydney, NSW 2052, Australia

KEYWORDS reductive dehalogenation; kinetic isotope effect; compound-specific isotope analysis; groundwater contamination; chlorinated methanes; trichloromethane, remediation; biodegradation, Vitamin B_{12}, *Dehalobacter* sp. strain UNSWDHB, *Dehalobacter* sp. strain CF

Abstract

Trichloromethane (TCM) is a frequently detected and persistent groundwater contaminant. Recent studies have reported that two closely related *Dehalobacter* strains (UNSWDHB and CF) transform TCM to dichloromethane, with inconsistent carbon isotope effects ($\varepsilon^{13}C_{UNSWDHB}$ = -4.3 ± 0.45‰; $\varepsilon^{13}C_{CF}$ = -27.5 ± 0.9‰). This study uses dual element compound specific isotope analysis (C; Cl) to explore the underlying differences. TCM transformation experiments using strain CF revealed pronounced normal carbon and chlorine isotope effects ($\varepsilon^{13}C_{CF}$ = -27.9 ± 1.7‰; $\varepsilon^{37}Cl_{CF}$ = -4.2 ± 0.2‰). In contrast, small carbon and unprecedented inverse chlorine isotope effects were observed for strain UNSWDHB ($\varepsilon^{13}C_{UNSWDHB}$ = -3.1 ± 0.5‰; $\varepsilon^{37}Cl_{UNSWDHB}$ = 2.5 ± 0.3‰) leading to opposing dual element isotope slopes (λ_{CF} = 6.64 ± 0.14 vs. $\lambda_{UNSWDHB}$ = -1.20 ± 0.18). Isotope effects of strain CF were identical to experiments with TCM and Vitamin B_{12} ($\varepsilon^{13}C_{Vitamin\ B12}$ = -26.0 ± 0.9‰, $\varepsilon^{37}Cl_{Vitamin\ B12}$ = -4.0 ± 0.2‰, $\lambda_{Vitamin\ B12}$ = 6.46 ± 0.20). Comparison to previously reported isotope effects suggests outer-sphere-single-electron transfer or S_N2 as possible underlying mechanisms. Cell suspension and cell free extract experiments with strain UNSWDHB were both unable to unmask the intrinsic KIE of the reductive dehalogenase (TmrA) suggesting that enzyme binding and/or mass-transfer into the periplasm were rate-limiting. Non-directed intermolecular interactions of TCM with cellular material were ruled out as reason for the inverse isotope effect by gas/water and gas/hexadecane partitioning experiments indicating specific, yet uncharacterized interactions must be operating prior to catalysis.

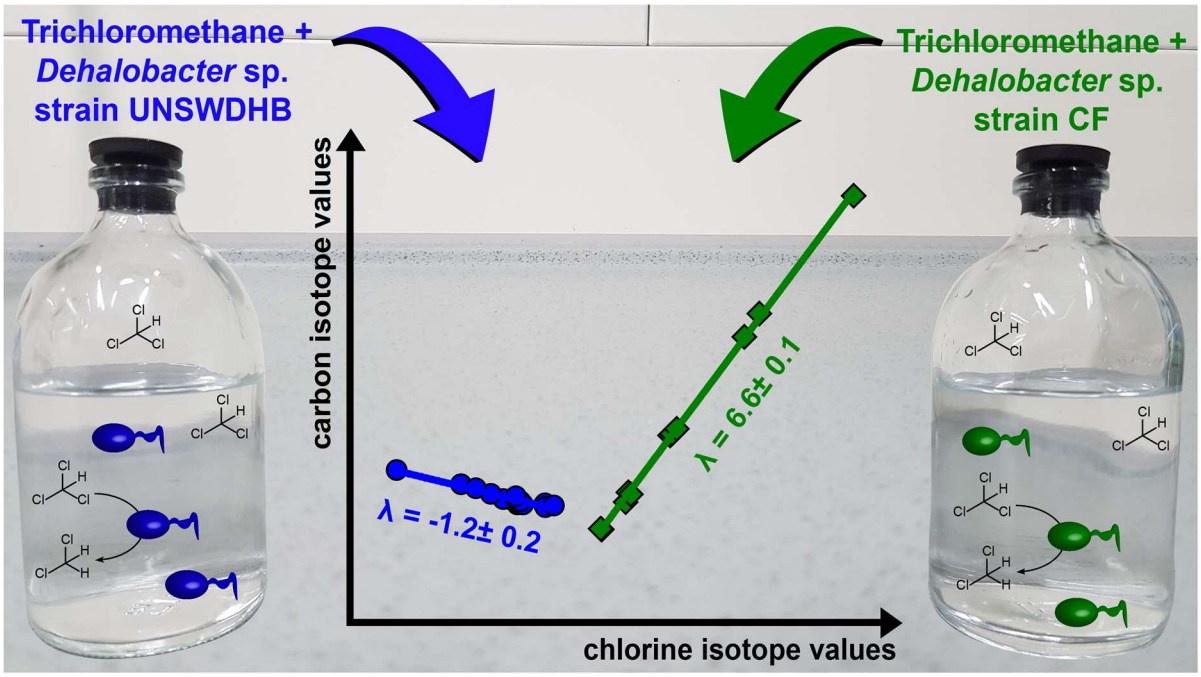
Trichloromethane +
Dehalobacter sp.
strain UNSWDHB
Trichloromethane +
Dehalobacter sp.
strain CF
carbon isotope values
chlorine isotope values
λ = -1.2± 0.2
λ = 6.6± 0.1

47

48

49

Introduction

Chloroform (IUPAC name trichloromethane (TCM)) is of natural and anthropogenic origin and was used as degreasing agent, precursor to Teflon and various refrigerants and used in medicine as an anesthetic[1, 2]. TCM is a common groundwater pollutant because of its extensive industrial production coupled with improper handling and disposal practices. It ranks 11th on the US-EPA list of hazardous substances, and is present at approximately 25% of the priority sites listed by the US-EPA[3].

TCM is a dense non-aqueous phase liquid (DNAPL) with a specific gravity of 1.49 (20°C) and water solubility of 8.1 g/L (25°C). When discharged into the environment, pure phase TCM descends into anoxic subsurface environments where it slowly dissolves into the surrounding groundwater over many years. In anoxic environments, TCM can be used as terminal electron acceptor by organohalide respiring bacteria (ORB). ORB therefore contribute to the natural attenuation of TCM: they can be specifically deployed, or *in situ* populations can be stimulated as an attractive remediation strategy [4].

TCM respiration to dichloromethane (DCM) by *Dehalobacter* sp. strains CF and UNSWDHB and *Desulfitobacterium* sp. strain PR has recently been described in laboratory studies[5-11]. Both *Dehalobacter* strains are strictly hydrogenotrophic while strain PR can use pyruvate as well as hydrogen as electron donors for TCM reduction. It has also been shown that strain UNSWDHB cannot utilize TCM under non-respiratory conditions (i.e. in the absence of hydrogen)[12]. In addition to TCM these ORB can also use 1,1,1- and 1,1,2-trichloroethane (TCA) as terminal electron acceptors. Strains UNSWDHB and PR can also utilize 1,1-dichloroethane (DCA). Strain UNSWDHB originates from a TCM contaminated site, whereas strains CF and PR hale from sites impacted with 1,1,1-TCA (aka methyl chloroform) [11, 13].

The reductive dehalogenases (RDase) responsible for TCM and chlorinated ethane reductive dechlorination are TmrA, CfrA and CtrA in strains UNSWDHB, CF and PR respectively, they

share >95% amino acid identity[7]. The small difference in amino acid composition has led to varying substrate affinity and enzyme kinetics for TCM, 1,1,1-trichloroethane 1,1,2-trichloroethane and 1,1-dichloroethane in all three RDases[7]. A common feature of RDases is that they contain a cobamide at the core of their catalytic site facilitating electron transfer for reductive dehalogenation reactions[14]. Amino acid residues around the active site dictates the enzyme's substrate affinity and specificity[7, 15]. The exact nature of the underlying biochemical reaction mechanisms, and whether the different substrate affinity and selectivity observed in TmrA and CfrA is reflected in unique features of either enzyme reaction is unknown.

Different enzymatic reaction mechanisms can lead to the same products and would, therefore not be recognized with conventional analysis. If they are associated with different isotope effects, however, compound-specific isotope effect analysis (CSIA) offers the opportunity to make differences in reaction mechanisms visible, and can at best case even elucidate the underlying reaction chemistry, as was recently shown for chlorinated ethene dehalogenation by Vitamin B_{12} [2, 16-21]. Here, carbon ($^{13}C/^{12}C$) and chlorine isotope ratios ($^{37}Cl/^{35}Cl$) are measured in TCM at natural isotopic abundance and reported relative to an international reference material:

$$\delta^{13}C = \frac{^{13}C/^{12}C_{Sample} - ^{13}C/^{12}C_{Reference}}{^{13}C/^{12}C_{Reference}} \quad (1)$$

$$\Delta\delta^{13}C = \delta^{13}C - \delta^{13}C_{initial} \quad (2)$$

Where $(^{13}C/^{12}C)_{Sample}$ and $(^{13}C/^{12}C)_{Reference}$ are isotope ratios of a TCM sample, taken during a biochemical reaction, and of an international reference material, respectively. $\delta^{13}C$ and $\delta^{13}C_{initial}$ are the isotope values of samples taken at a specific time point and at the beginning of the reaction, respectively. Compound-specific isotope effects are subsequently evaluated according to the Rayleigh equation[22, 23]:

$$\delta^{13}C = \delta^{13}C_{initial} + [\varepsilon^{13}C \cdot \ln f] \quad (3)$$

Where *f* is the fraction of the remaining substrate at any given time relative to the starting concentration. $\varepsilon^{13}C$ is the isotopic enrichment factor that expresses the difference in reaction rates of light (^{12}k) vs. heavy isotopologues (^{13}k) and is the equivalent to the kinetic isotope effect (KIE); KIE = $^{12}k/^{13}k$. In most cases, a "normal" isotope effect is observed where light isotopes react faster than heavy isotopes. In rare cases heavy isotopes can react faster, corresponding to an "inverse" isotope effect, for example for ^{15}N during degradation of atrazine by *Chelatobacter heintzii*, *Pseudomonas sp*. ADP, and *Arthrobacter aurescens* TC1[24] or ^{2}H for degradation of TCE by a mixed *Dehalococcoides* culture [25].

Recently, the analysis of chlorine isotope ratios has become possible enabling the construction of dual element isotope plots (e.g. $\Delta\delta^{13}C$ vs $\Delta\delta^{37}Cl$) [26]. The resultant slope $\lambda = \Delta\delta^{13}C/\Delta\delta^{37}Cl \approx \varepsilon^{13}C/\varepsilon^{37}Cl$ relates the isotope effects of the two elements to each other and provides a more sensitive parameter to differentiate reaction mechanisms than isotope effects from one element alone [27-31]. An additional advantage of dual element isotope slopes is that they are remarkably insensitive towards masking of intrinsic isotope effects that occurs when the bond breaking reaction is not rate limiting in biocatalysis. If an additional reaction step (e.g. diffusion through the cell membrane or binding of a substrate to an enzyme) is partially rate limiting, but does not cause isotope fractionation itself, changes of isotope ratios in both elements are reduced in the same proportion so that the slope of λ remains the same even if ε values are smaller.[27, 32, 33]

While first reports on carbon isotope fractionation associated with TCM biodegradation revealed differences between strain UNSWDHB ($\varepsilon^{13}C = -4.3 \pm 0.45‰$) and strain CF ($\varepsilon^{13}C = -27.5 \pm 0.9‰$) [5, 8], data on chlorine isotope fractionation are yet to be reported. This raises the questions (i) what features of the enzyme reaction cause this different isotope fractionation (i.e., C-Cl bond cleavage vs. masking by mass transfer vs. isotope effects of other steps in the enzyme reaction); (ii) what underlying reaction mechanism lies at the heart of TCM respiration and

whether this mechanism can be mimicked with the cofactor cyanocobalamin alone; (iii) whether such a mechanism can explain why TCM respiration stalls at the stage of DCM [5, 7, 8, 11] .

To address these questions, we investigated both carbon and chlorine isotope effects in TCM transformation by strains UNSWDHB and CF. Furthermore, the isotope effects of TCM dechlorination by the RDase cofactor Vitamin B_{12}, strain UNSWDHB cell suspensions and crude protein extracts were also monitored. Additionally, in order to understand potential binding isotope effects originating from non-covalent interactions of the chlorine atoms in TCM during enzyme catalysis, equilibrium chlorine isotope effects were independently determined for gas/water and gas/hexadecane partitioning. Isotope effects were compared to previously reported isotope fractionation data and possible mechanistic explanations were considered.

Experimental Procedures

TCM dechlorination via respiring CF and UNSWDHB cells and UNSWDHB cell-free extracts

A mixed culture, DHB-CF/MEL, containing the TCM respiring strain CF was grown in triplicate 2 L cultures in a defined mineral medium[34] in an anaerobic chamber. The culture flasks were sealed with blue butyl septa (Bellco, 20mm, part # 2048-11800 and TCM was supplied to a final concentration of 1 mM in solution (aqueous phase nominal concentration) with ethanol and lactate provided as electron donors. Strain UNSWDHB was grown in triplicate 2 L cultures in anaerobic bicarbonate-buffered mineral medium as previously described[7]. The culture flasks were sealed with Teflon-faced septa (Wheaton, 20 mm, part # 224100-175) and TCM was supplied to a final concentration of 1 mM in solution. Over the course of TCM degradation by strains CF and UNSWDHB, aqueous samples for CSIA analysis (4 mL) were withdrawn from the culture flasks with a glass syringe and transferred to a 5 mL glass vial such

147 that it was completely filled and contained 1 mL of sulfuric acid (1 mM) (i.e. no headspace).
148 The vials were sealed with Teflon-faced septa (Wheaton, 20 mm, part # 224100-175).
149 *Analysis of TCM and DCM in strain CF cultures.* The aqueous phase concentration of TCM
150 and DCM was measured via manual headspace analysis using a Hewlett-Packard 5890 Series
151 II GC-FID equipped with an Agilent GSQ column (30 m x 0.53 mm). Headspace samples (300
152 μL) were taken directly from the headspace of culture flasks using a pressure lockable gastight
153 syringe. The GC inlet was operated in splitless mode at 250°C. The oven temperature was
154 ramped up from 50°C to 155°C at 30°C/min, and then from 155°C to 180°C at 4°C/min.
155 *Analysis of TCM and DCM in strain UNSWDHB cultures.* The aqueous phase concentration of
156 TCM and DCM was measured via manual headspace analysis using an Agilent 7890 GC-FID
157 equipped with an Agilent GSQ column (30 m x 0.32 mm). Headspace samples (100 μL) were
158 taken directly from the headspace of culture flasks using a pressure lockable gastight syringe.
159 The GC inlet was operated in split mode at 250 °C. The oven temperature was ramped from an
160 initial temperature of 150°C to 250°C at 30°C/min.
161 *Cell harvesting for biochemical TCM dechlorination assays.* UNSWDHB cells were harvested
162 as previously described[7] . Where possible the procedure was performed in an anoxic chamber
163 as described below. Aliquots of UNSWDHB culture (50 mL) with a cell density of ~ 10^7 cells
164 per mL were transferred to anoxic 50 mL screw cap plastic centrifuge tubes. The thread of the
165 tube was modified with PVC adhesive tape to ensure anoxic conditions. Outside the chamber,
166 the tubes were centrifuged at 10000 x g for 20 mins at 4 ° C. Back in the chamber the
167 supernatant was decanted and the remaining cell pellet was resuspended in anoxic Tris/HCl-
168 buffer (50 mM, pH 7) containing Ti(III) citrate (1 mM), centrifuged again and the supernatant
169 was discarded. The cell pellet was finally resuspended in tris-buffer (5 mL) containing Ti(III)
170 citrate (2 mM) and methyl viologen (2 mM). The cells were immediately used in activity assays.
171

172 *Preparation of cell extracts for biochemical TCM dechlorination assays.* In an anoxic chamber
173 cell suspensions (1.5 ml, ~10^8 cells) as described above were transferred to 2 mL cryo tubes
174 containing 20 mg of glass beads (1.0 mm diameter) and they were bead-beaten for 5 min at 30
175 Hz (Qiagen, TissueLyser II). After bead beating, the tubes were centrifuged at 16000 x g (10
176 min, 4 °C). The samples were then transferred back into the anoxic chamber where the
177 supernatants were filtered through a 0.22 micron filter (Millipore) to ensure that no intact cells
178 remained. The cell extracts were used immediately in activity assays. The concentration of
179 protein per ml was calculated to be ~20 $\mu g.ml^{-1}$ [(7)].
180
181 *TCM dechlorination by suspended cells or cell lysate.* In an anoxic chamber 7 x 4 mL of cell
182 suspension or cell lysate amended with electron donors titanium citrate (2 mM) and methyl
183 viologen (1 mM) were transferred to 7 x 5 mL headspace vials and then crimp-sealed with
184 Teflon faced rubber septa. The reaction was initiated by the addition of 1 mL of a 5 mM TCM
185 solution in Tris/HCl-buffer (50 mM, pH 7) such that the final concentration of TCM was 1 mM.
186 The vials were incubated in the anoxic chamber, at 30 °C. At regular intervals a reaction was
187 terminated by withdrawing 1 mL and replacing it with sulfuric acid (1 M, 1 mL). The withdrawn
188 cell suspension or cell lysate was transferred to a 10 ml headspace flask and analyzed for TCM
189 and DCM by GC-FID. The acidified contents of the 5 mL vial were analyzed by CSIA.
190
191 *Analysis of TCM and DCM in strain UNSWDHB suspended cell and cell lysate experiments.*
192 Quantification of the aqueous phase concentration of TCM and DCM was performed on a
193 Shimadzu 2010 GC equipped with a headspace Autosampler (PAL LHS2-xt-Shim). The GC
194 column and parameters were identical to those described above for strain UNSWDHB. The
195 headspace flasks were agitated (200 rpm) at 80°C for 5 minutes before 500 µl of the vial
196 headspace was injected into the GC inlet.
197

198 *Calibration standards for TCM and DCM analysis in CF and UNSWDHB cultures and*
199 *biochemical assays*
200 Calibration standards ranging from 0.2 to 2 mM (nominal) were prepared in 260 mL culture
201 flasks with 200 mL of water. Gas phase and headspace concentrations of TCM and DCM were
202 calculated by Henry's Law using dimensionless constants 0.182 and 0.110 respectively. These
203 values were obtained from the US-EPA (https://www3.epa.gov/ceampubl/learn2model/part-
204 two/onsite/esthenry.html).
205
206 **TCM dechlorination by Vitamin B_{12} at pH 6.5.**
207 *Preparation of buffered TCM solution* **(solution 1)**. Water (95 mL) and sodium carbonate (0.6
208 g 5.7 mmol; 60 mM) were added to a 100 mL bottle equipped with a stirrer. The pH was
209 adjusted to 6.5 with 1 M HCl or 1 M NaOH and the solution was deoxygenated by nitrogen
210 with purging. The solution was then transferred into an anoxic glovebox (MBRAUN; LABstar,
211 Munich, Germany) where TCM (48 µL; 0.59 mmol; 6.2 mM) was added.
212 *Preparation of Ti(III)citrate solutions* **(solution 2)**. A titanium citrate solution was prepared by
213 adding 7.5 mL of a ~15% titanium (III) chloride solution (9 mmol; 1.18 M) to a 100-mL two-
214 necked flask equipped with a stirrer. The solution was diluted with 15 mL of water resulting in
215 a Ti(III) concentration of approximately 400 mM. The solution was sparged with nitrogen and
216 anoxic conditions were maintained throughout the entire preparation. Sodium citrate (4.9 g;
217 16.6 mmol; 740 mM) was then added to this solution together with 1.5 g (14 mmol; 63 mM)
218 carbonate buffer and the pH was adjusted to 6.5 with sodium carbonate.
219 *Preparation of bottles containing Vitamin B_{12}*. To a 60 mL vial equipped with magnetic stir bar,
220 10 mg (0.007 mmol in 35 mL; 21µM) of Vitamin B_{12} was added together with 35 mL of the
221 buffered TCM solution (**solution 1)** in an anoxic glovebox (MBRAUN; LABstar, Munich,
222 Germany). The vial was closed with a Mininert^{TM} valve (Valco Instruments Co. Inc.; Houston;
223 USA) and the reaction was started by adding 5 mL of the titanium citrate solution (**solution 2**).

The final concentration of TCM in the reaction solution was 5.4 mM (0.22 mmol). Headspace samples (0.1 mL) were withdrawn from the headspace through the Mininert^{TM} caps of the bottles in regular intervals with a pressure lockable gas-tight syringe. For all sample concentrations, carbon- and chlorine isotope measurements were conducted (see below). For calibration, standards ranging from 0.5 to 6 mM were prepared in 60 mL vials with 40 mL of water.

Concentration measurements of TCM and reaction products in TCM dechlorination by Vitamin B_{12}. The reaction of TCM with Vitamin B_{12} was evaluated by gas chromatography/mass spectrometry (GC/MS) analysis with manual injection of 0.1 mL headspace samples using a Pressure lock syringe. Samples were injected into an Agilent 7890A GC coupled to an Agilent 5975C quadrupole MS. The column was a 60 m Q-Plot (Agilent, Santa Clara, California) column of 0.32 mm inner diameter operated with a helium carrier gas flow of 1.6 mL/min. The injector temperature was 250 °C and the temperature program of the GC started at 40 °C for 9 min, was ramped at 15 °C/min to 53°C for 2.7 minutes, then ramped at 13°C/min to 134°C, ramped again at 20°C to 200°C and finally held at 200 °C for 23 min. Concentrations were calculated using a 10-point calibration curve. Gas phase and headspace concentrations of TCM and DCM were calculated by Henry's Law using dimensionless constants 0.150 (at 298.15 Kelvin) and 0.099 (at 298.15 Kelvin) respectively.

Compound-specific Isotope Analysis

Stable Carbon Isotope Analysis. For carbon isotope analysis headspace samples were manually injected through a pressure lock syringe or automatically by High Dynamic (HD) type syringe into a gas chromatograph-isotope ratio mass spectrometer (GC-IRMS) system (Thermo Fisher Scientific, Waltham, Massachusetts, USA) consisting of a Trace GC coupled to a MAT 253 IRMS through a GC/C III combustion interface. The GC was equipped with a 60 m Q-Plot column of 0.32 mm inner diameter (Agilent, Santa Clara, California). The GC program started

at 40 °C for 9 min, was ramped at 15 °C/min to 53°C for 2.7 minutes, then ramped at 13°C/min to 134°C, ramped again at 20°C to 200°C and finally held at 200 °C for 23 min. After separation, the compounds were combusted to CO_2 and the $^{13}C/^{12}C$ ratio was determined from the amount of $^{13}CO_2/^{12}CO_2$ molecules. Delta values relative to the Vienna Pee Dee Belemnite (VPDB) international standard were directly derived from the instrument software where calibrated monitoring gas was measured against the samples. As quality control, an external standard of $CHCl_3$ ($\delta^{13}C$ of -48.4‰ ± 0.2‰) that had been characterized by EA-IRMS was run along with the samples. The overall analytical uncertainty 2σ of carbon isotope measurements was ± 0.5‰.

Stable Chlorine Isotope Analysis. Chlorine isotope analysis was performed according to Heckel et al. 2017 [26]. For chlorine isotope measurements headspace samples were injected into the GC-IRMS system (Thermo Scientific, Waltham, Massachusetts, USA), using a pressure lock syringe (for manual injection) or a HD type syringe (for automated injection). The GC-IRMS consisted of a Trace GC that was connected to a MAT 253 IRMS with dual inlet system via a heated transfer line. The GC was equipped with a 30 m VOCOL column (Supelco, Bellefonte, Pennsylvania, USA) with 0.25 mm inner diameter, a film thickness of 1.5 µm and operated with a He carrier gas flow of 1.4 mL/min. The GC program started at 60°C (2.0 min), increasing at 8°C/min to 165 °C and at 25 °C/min to 220 °C (1.0 min). After separation, chloroform was directly transferred into the IRMS and fragments 48 and 50 were analyzed to determine the $^{37}Cl/^{35}Cl$ ratio[26]. In the first step instrument chlorine isotope values were derived through the instrument's software, where monitoring gas was measured against the samples in each run. Subsequently, these instrument isotope values $\delta^{37}Cl$ were subjected to an external two-point calibration relative to the international reference Standard Mean Ocean Chloride (SMOC) according to Bernstein et al. [35] by daily measurements of external standards of $CHCl_3$ with a chlorine isotope signature ($\delta^{37}Cl$) of -3.02‰ and -5.41‰ [26]. The analytical uncertainty 2σ of chlorine isotope measurements was ±0.2‰.

Calculation of the Apparent Kinetic Isotope Effect (AKIE)

ε values, which are calculated according to the Rayleigh equation (equation 3), reflect an average over all molecular positions. To infer bond-specific isotope effects, AKIE values may be estimated, which can be useful to compare observable isotope fractionation to that in other substances and reaction mechanism. AKIE values can be calculated by equation 4 and 5:

$$\varepsilon_{rp} \approx \frac{n}{x} \cdot \varepsilon_{bulk} \quad (4)$$

$$AKIE_{C,Cl} = \frac{1}{z \cdot \varepsilon_{rp} + 1} \quad (5)$$

ε_{rp} is the isotopic fractionation at the reacting position, n is the number of atoms of the investigated element, x is the number of reactive positions and z describes the number of identical reactive sites. For chloroform $n_C = x_C = z_C = 1$ and $n_{Cl} = x_{Cl} = z_{Cl} = 3$ when a C-Cl bond is cleaved (primary isotope effect) whereas $n_{Cl} = x_{Cl} = 3$, $z_{Cl} = 1$ when in the rate-determining step all C-Cl bonds remain intact (secondary isotope effect).

Experimental Determination of Chlorine Isotope Effects in Air-Water & Air-Hexadecane Partitioning.

To exclude co-solvent effects in the partitioning experiments the total amount of TCM should not exceed 0.1% of the total amount of solvent[36]. Therefore, to prepare the starting solution for the air-water partitioning experiment a 40 mL vial equipped with a stirrer was completely filled with water to avoid air bubbles during mixing and 200 mg TCM were added to produce a 5 g/L (38 mM) solution. For the air-hexadecane partitioning experiment a smaller nominal concentration was chosen to account for the smaller molar density of hexadecane: 2.7 µL (4.1 mg; 0.018 mmol.) TCM was added to a 10 mL vial containing a stirrer and 10 mL of hexadecane resulting in a TCM concentration of 3.4 mM. Vials were closed by Mininert screw caps and the solutions were rigorously stirred for 48 h to ensure complete dissolution. To ensure that all of

299 the TCM was dissolved, liquid samples were taken and the final concentration was validated
300 by GC-qMS. Water-air and hexadecane-air partitioning experiments were conducted in
301 modified ND18 headspace vials (Figure S1). The vials consisted of two parts which were
302 separated by tapered grinding (2 cm from the bottom) leading to an upper part of ~14 mL and
303 a lower part of ~4 mL. The two parts were connected through an aperture in the tapered
304 grinding, which could be closed when a metal ball (stainless steel, diameter: 0.9 cm) located
305 into place driven by gravity. In contrast, the aperture could be opened when the ball was drawn
306 away by application of magnetic force or by centrifugal force when the vial was agitated. For
307 the experiments, the lower part of the vial was filled with an aliquot of the starting solution
308 (Figure S1), the metal ball was added, and the system was closed with a screw cap (1.3 mm
309 silicone/PTFE septum, 45°, Carl Roth, Karlsruhe, Germany). The aliquot of the starting solution
310 to be added was calculated to accomplish a 50:50 distribution by mass between the headspace
311 and the condensed phase. The distribution (in %) between two equilibration steps n was
312 calculated according to:
313
314 $$distribution = \frac{peak\ area_n - peak\ area_{n-1}}{peak\ area_n} \quad (6)$$
315
316 For air-water partitioning 1 mL of the TCM starting solution was added to the vial and 0.05 mL
317 for the air-hexadecane partitioning, respectively. After equilibration in the autosampler agitator
318 (speed: 500 rpm, incubation temperature: 33 °C, equilibration time: 60 min) the metal ball
319 closed the hole and headspace samples were taken manually. Afterwards, the vial was opened,
320 the gas phase was exchanged with a gentle nitrogen stream for 20 s and the vial was quickly
321 closed with a new screw cap. Experiments were performed in triplicate. To ensure that the
322 system is leak proof, we prepared six modified vials where three of them were agitated for one,
323 three and 24 hours, respectively. Headspace samples were taken from each vial and measured
324 with the GC-qMS. No change of the mass balance was observed.

Results and Discussion

Comparison of biotic TCM transformation by strain UNSWDHB and strain CF reveals opposing dual element isotope trends

Previous work studying stable isotope fractionation of TCM in organohalide respiration was confined to carbon only, and performed with cultured cells [5, 8]. In these recent studies TCM transformation by the two closely related strains CF and UNSWDHB gave significantly different ^{13}C isotope enrichment factors ($\varepsilon\ ^{13}C$ = -27.5 ± 0.9‰ and $\varepsilon\ ^{13}C$ = -4.3 ± 0.45‰, respectively).

To further understand stable isotope fractionation of TCM during its respiration by strains UNSWDHB and CF, reductive dehalogenation experiments with cultured cells of both strains were again conducted. On this occasion fractionation of stable chlorine isotopes were also monitored. Pronounced carbon isotope effects ($\varepsilon\ ^{13}C$ = -27.91‰ ± 1.66‰; $AKIE_C$ = 1.028 ± 0.002; Figure 1a) were observed in transformation by strain CF which are similar to the carbon isotope effects previously reported[8]. Remarkably, the pronounced carbon isotope fractionation was accompanied by large chlorine isotope fractionation ($\varepsilon\ ^{37}Cl$ = -4.20‰ ± 0.26‰; $AKIE_{Cl}$ = 1.013 ± 0.001; Figure 1b).

A contrasting isotope fractionation pattern was observed for TCM dechlorination by strain UNSWDHB, where small carbon isotope effects were accompanied by surprising inverse chlorine isotope effects ($\varepsilon^{13}C$ = -3.07 ± 0.53‰; $AKIE_C$ = 1.003 ± 0.001; $\varepsilon\ ^{37}Cl$ = 2.52 ± 0.34‰; $AKIE_{Cl,\ primary}$ = 0.992 ±0.001; $AKIE_{Cl,\ secondary}$ = 0.997 ± 0.0005, Figure 1a, b). The contrast can be further expressed in dual element isotope plots, where the resultant slopes (λ) have opposite trends ($\lambda_{\ UNSWDHB}$ = -1.20 ± 0.18 vs. $\lambda_{\ CF}$ = 6.64 ± 0.14; Figure 1c). AKIE values can be put into perspective by comparison with maximum calculated Streitwieser Limits [23]. The $AKIE_C$ value for the reduction of TCM by strain CF is in the range of typical carbon isotope effects[23]

suggesting that the C-Cl bond cleavage is not masked and, therefore, represents the rate-determining step. The AKIE value for chlorine, furthermore, is also indicative of a C-Cl bond cleavage with an $AKIE_{Cl}$ of 1.013 being close to the calculated Streitwieser Limit of 1.013 [23].

In the case of TCM dehalogenation by strain UNSWDHB, in contrast, both carbon and chlorine AKIEs are much lower than the Streitwieser Limit. This indicates that the intrinsic KIE is masked, and therefore the C-Cl bond cleavage is not rate-determining. Hence, observed isotope effects are likely indicative of a rate-determining step prior to the C-Cl bond cleavage.

Similar carbon and chlorine isotope effects for dehalogenation of TCM by Vitamin B12 and *Dehalobacter* strain CF provide evidence of a common reaction mechanism

To gain deeper insight into the dehalogenation processes, the investigated system was simplified by using only the RDase cofactor Vitamin B_{12} for TCM reduction. Cobamides, such as Vitamin B_{12}, reside at the core of RDases[15] and are a well-documented model system to investigate reductive dehalogenation mechanisms[18, 20, 30]. For the reductive dehalogenation of TCM by Vitamin B_{12} pronounced "normal" carbon and chlorine isotope fractionation was observed ($\varepsilon\ ^{13}C = -26.04 \pm 0.91‰$; $\varepsilon\ ^{37}Cl = -4.00 \pm 0.20‰$; $\lambda = 6.46 \pm 0.20$; Figure 1) that was identical to the results from TCM reduction by strain CF. This agreement provides strong evidence that both systems share a common reaction mechanism and that, in the case of strain CF, the observed isotope effects reflect the reaction step with the cobamide cofactor located within the responsible RDase. This raises questions: (i) which step is masking the carbon-chlorine bond cleavage in the case of strain UNSWDHB, and (ii) what is /are the reason(s) for the inverse chlorine isotope effect(s).

Organohalide respiration by *Dehalobacter* cells is a complex process with many steps prior to C-Cl bond cleavage including TCM and hydrogen diffusion to the cell, hydrogen oxidation,

menaquinone reduction and oxidation[12, 37]. Any of these steps could be rate-limiting. The complexity of the system can be significantly reduced in abiotic resting cell activity assays where methyl viologen is employed as an artificial electron donor that directly reduces the cobamide cofactor in the TmrA[38]. Furthermore, rate-limiting steps involving the diffusive transport of TCM to the active site could be effective including: 1. Transport through the cell membrane, 2. Interactions with cellular structures and, 3. Binding interactions with TmrA prior to C-Cl bond cleavage [39]. The potential rate-limiting steps 1 and 2 could be negated in activity assays with crude protein extracts of strain UNSWDHB.

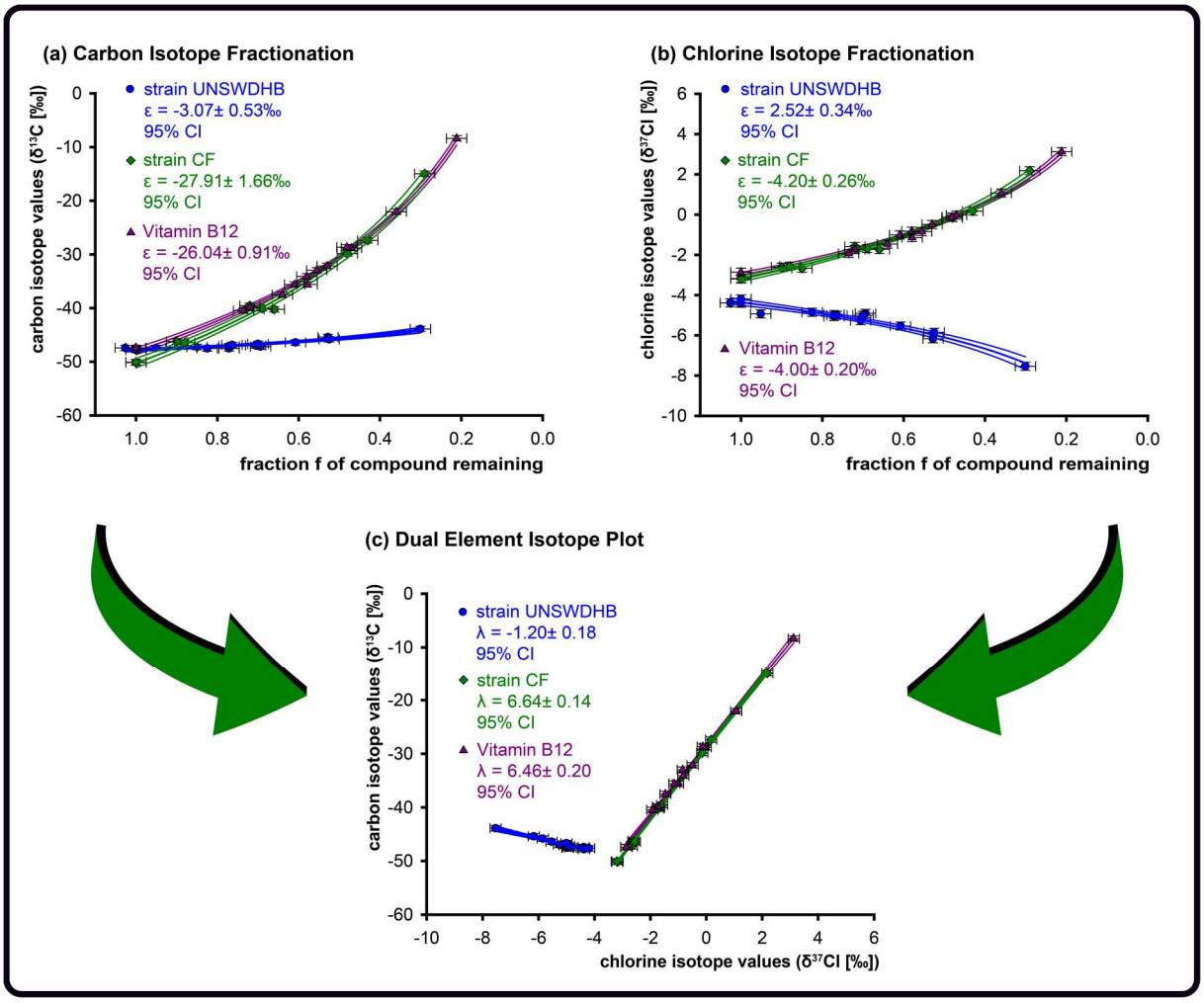

Figure 1: Comparison of the isotopic enrichment factors ε of carbon (a) and chlorine (b) of TCM transformation by strains UNSWDHB and CF and Vitamin B12 were obtained by fitting changes in isotope values against the remaining fraction of substrate. (c) By combining changes in chlorine and carbon isotope values dual element isotope slopes are generated. Error bars

reflect the analytical uncertainty of 2.5% for concentration measurements, 0.2‰ for chlorine and 0.5‰ for carbon measurements.

TCM transformation by strain UNSWDHB cell suspensions, crude protein extracts and the enzymatic cofactor Vitamin B12

In an attempt to unmask the intrinsic KIE of TCM dechlorination by strain UNSWDHB, abiotic activity assays where performed using both intact suspended cells and crude protein extracts of strain UNSWDHB (Figure 2a-c). Significantly different TCM to DCM reaction rates were observed in the three systems [k^{-1} (growth conditions) = (6.2 ± 6) x 10^{-3} h^{-1}; k^{-1} (cell suspension) = 3.8 ± 0.4 h^{-1}; k^{-1} (crude protein extract) = 0.20 ± 0.07 h^{-1}] (Figure 2a-c). These differences are likely due to the lower cell density under growth conditions (~1 x 10^5 cell ml^{-1} at time zero) compared with ~1 x 10^8 cell per ml^{-1} under suspended cell conditions, and also the effect of methyl viologen directly reducing TmrA in cell suspension and cell free extract experiments. In experiments using Vitamin B_{12}, dehalogenation of TCM to methane was achieved (Figure 2d). All investigated systems presented a mass balance > 90%. Furthermore, while monitoring the carbon isotope values of TCM during its attenuation we also recorded the isotope changes in all transformation products (i.e. DCM, chloromethane and methane) and we were able to preserve a closed carbon isotope mass balance over the whole reaction (Figure S2).

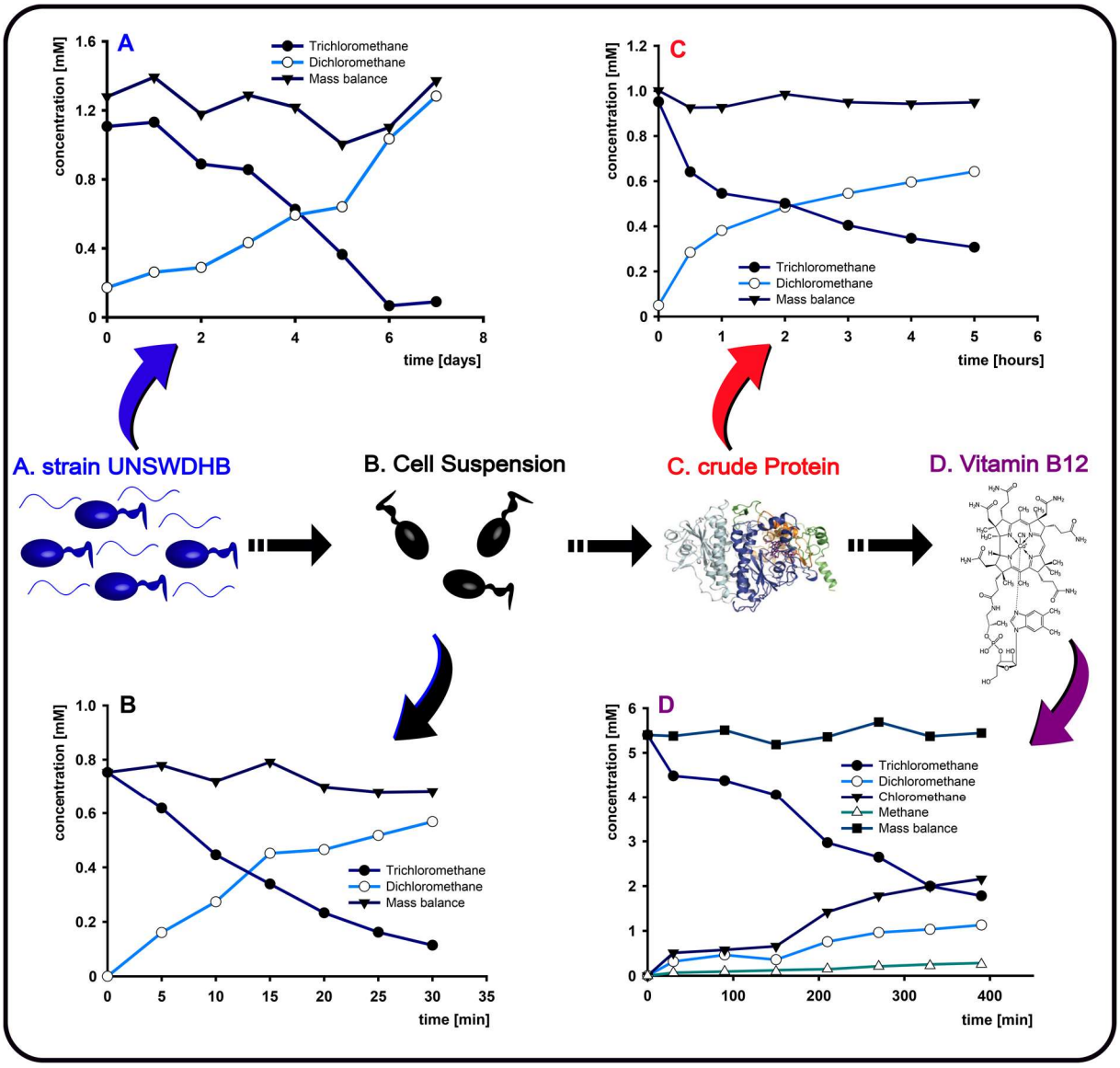

405

406 **Figure 2:** TCM transformation by **A.** Respiring cells (strain UNSWDHB); **B**. Cell Suspensions;
407 **C.** Crude protein extracts and **D.** Vitamin B12 and respective product development

408

409 **Identical normal carbon but different inverse chlorine isotope effects in TCM**
410 **transformations by respiring cells, cell suspensions and crude protein extracts**

411 Similar to cultured cells, small carbon isotope fractionation was observed for TCM
412 dehalogenation by cell suspensions ($\varepsilon\ ^{13}C$ = -2.68 ± 0.17‰; Figure 3a) and crude protein
413 extracts ($\varepsilon\ ^{13}C$ = -3.40 ± 0.30‰; Figure 3a). Inverse chlorine isotope effects were detected in
414 the three systems, increasing from the crude protein extract ($\varepsilon^{37}Cl$ = 0.78 ± 0.15‰; Figure 3b)
415 to cell suspensions ($\varepsilon\ ^{37}Cl$ = 1.46 ± 0.16‰; Figure 3b) to respiring cells ($\varepsilon\ ^{37}Cl$ = 2.52 ± 0.34‰;

Figure 1b and 3b). The respective dual element isotope plot (Figure 3c) illustrates significantly different slopes (95% confidence interval), with the steepest slope observed in TCM transformation by crude protein extract ($\lambda = -3.90 \pm 0.5$) and the shallowest by respiring cells ($\lambda = -1.20 \pm 0.18$). It is noteworthy that diffusion limitation was observed for the cell suspension experiments that were not continually agitated, resulting in smaller chlorine isotope effects (ε $^{37}Cl = 0.19 \pm 0.26$‰; Figure S3). Care was therefore taken during both cell suspension and cell extract experiments to ensure continual agitation (200 rpm) to avoid effects of diffusion limitation through aqueous solution.

Remarkably, within the systems (A) to (C) of Figure 3, the greatest carbon, but the smallest chlorine isotope effect was observed in the system with the lowest complexiy (i.e. the crude protein extract). This observation indicates that intrinsic features of TmrA must be responsible for this observed small inverse chlorine isotope fractionation, which reflect neither the reaction chemistry of Vitamin B_{12} nor the (larger) inverse isotope effect of whole cells. Potentially, either diffusion of the substrate into the substrate tunnel of the RDase (assuming it has one similar to *Sulfurospirillum multivorans* PceA [15]) or into the catalytic site could be rate-determining [40]. Given that the intrinsic KIE of the enzyme reaction is clearly masked by a rate-limiting step that causes small, but significant isotope fractionation of TCM, it is not possible to draw conclusions regarding the reaction mechanism involved in the C-Cl bond cleavage by TmrA.

The observation that inverse chlorine isotope enrichment factors diminished with decreasing reaction system complexity (i.e. respiring cells > suspended cells > crude protein extract) indicates that the steps prior to the enzyme reaction contribute to larger inverse chlorine isotope effects. The bacterium morphology may provide an explanation. Strain UNSWDHB is a gram-negative organism and the RDase resides on the cytoplasmic membrane facing the periplasmic

space[7, 41,12]. Based on this configuration, TCM has to pass through the outer membrane before diffusing through the periplasmic space to the RDase. Diffusion through the outer cell membrane or through periplasmic space can be excluded as origin of these inverse isotope effects because diffusion through any medium always leads to normal isotope effects [42, 43]. The additional inverse isotope effects, therefore, must be caused by molecular interactions of TCM with other cell material within the periplasmic space.

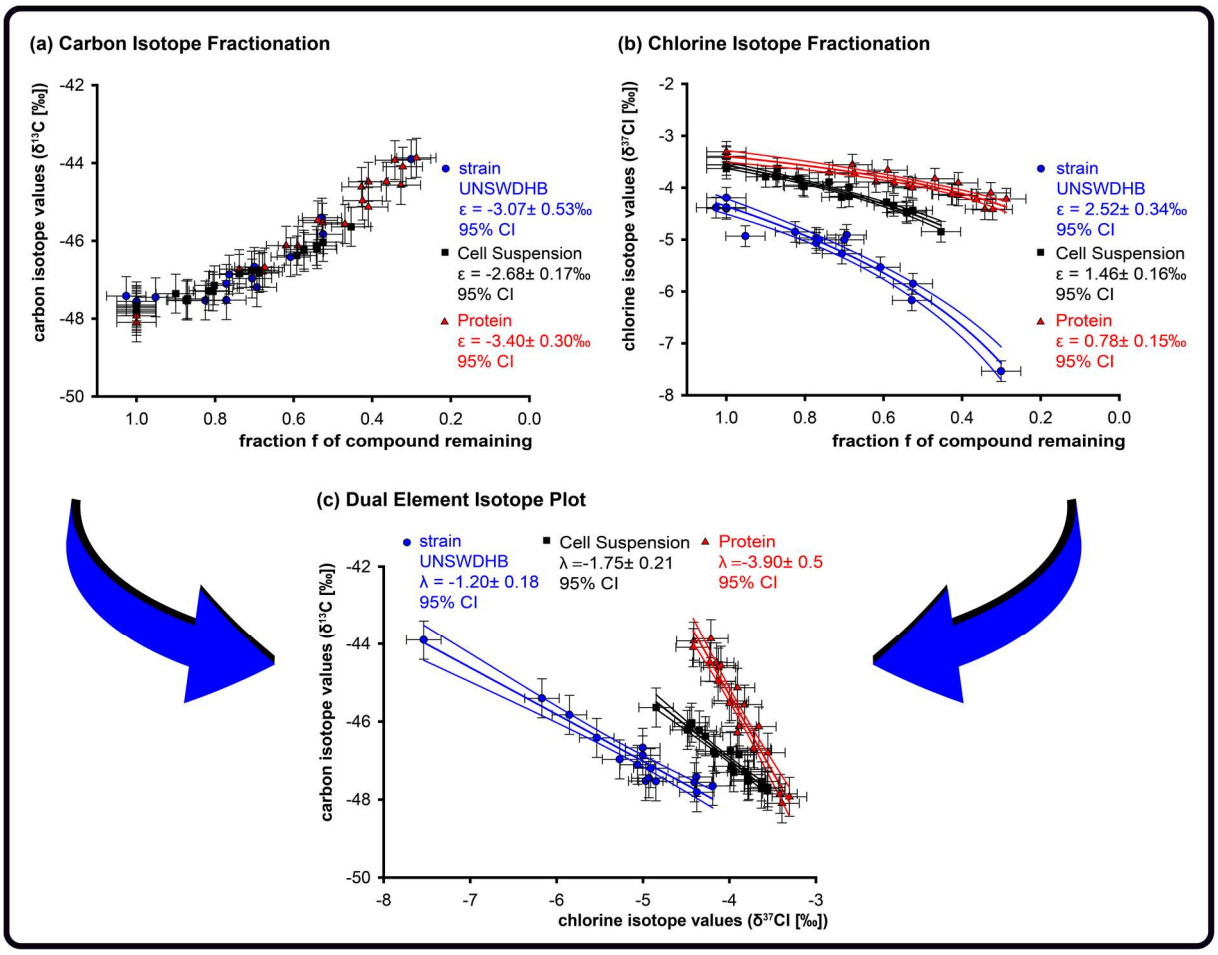

Figure 3: Isotopic enrichment factors ε of carbon (a) and chlorine (b) via TCM transformation by strain UNSWDHB, cell suspension and protein were obtained by fitting changes in isotope values against the remaining fraction of TCM. (c) Dual element isotope plots are gained by fitting changes in chlorine isotope values against changes in carbon isotope values. Error bars reflect the analytical uncertainty of 2.5% for concentration measurements, 0.2‰ for chlorine and 0.5‰ for carbon measurements.

Pronounced inverse isotope effects have been reported for nitrogen[24] and hydrogen [25, 44], however, to the best of our knowledge, no distinct inverse chlorine isotope effect associated

456 with organochlorine transformations have previously been reported . Inverse isotope effects are
457 normally observed, when the coordination environment of a target molecule becomes confined
458 leading to stiffer bending vibration[45, 46]. It is, therefore, possible that interactions of TCM
459 chlorine atoms with cellular material may lead to inverse isotope effects. Intermolecular
460 interactions between molecules, which can occur during these processes, are hydrogen-bridge
461 bonding or Van der Waals interactions. To examine whether these intermolecular interactions
462 can induce inverse chlorine isotope effects, partitioning experiments were performed for (a)
463 TCM partitioning between air (no intermolecular interactions) and water (combined effect of
464 hydrogen-bridge bonding and Van der Waals interactions) and (b) TCM partitioning between
465 air and hexadecane (only Van der Waals interactions). The same question had already been
466 addressed regarding changes in carbon isotope ratios of trichlorofluoromethane, TCM and
467 methanol[47], however, in an experimental setup where diffusive and equilibrium isotope effects
468 were at work simultaneously[48]. Here, we aimed to measure only the equilibrium isotope effects
469 of partitioning and, therefore, chose an experimental design where liquid and gas phases could
470 be brought into equilibrium and where the phases were subsequently separated by a metal ball
471 valve (Figure S1).

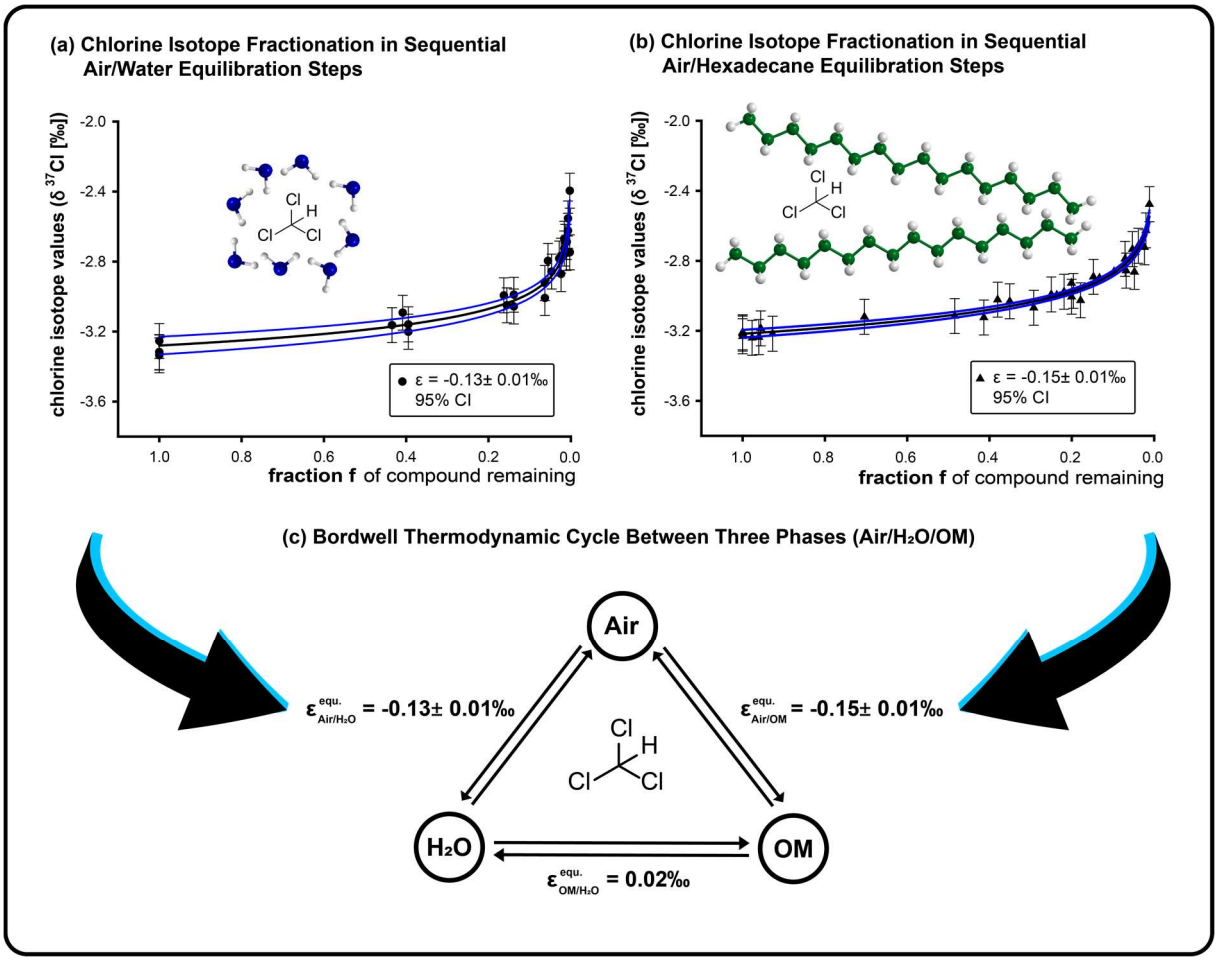

Figure 4: Chlorine isotope effects of equilibrium partitioning of (a) air/water and (b) air/hexadecane. (c) Bordwell thermodynamic cycle between air, H_2O and organic material (OM) phases. Error bars reflect the analytical uncertainty of 0.2‰ for chlorine measurements.

Water/air and hexadecane/air partitioning do not induce inverse chlorine isotope effects

The stepwise water/air partitioning resulted in a very small fractionation of ^{37}Cl in the remaining TCM (normal chlorine isotope effect; $\varepsilon\ ^{37}Cl = -0.13 \pm 0.1‰$; Figure 4a). This small, but significant normal isotope effect implies that new, intermolecular interactions were formed in the liquid phase whose additional modes overcompensated for the weakened molecular vibrations. At room temperature this phenomenon is typically observed for the formation of new hydrogen bonds as opposed to weaker van der Waals interactions[49, 50] (consider the normal vapour pressure isotope effect of water as opposed to inverse vapour pressure isotope effects of organic solvents). A nearly identical normal isotope effect was obtained, however, also for hexadecane/air partitioning ($\varepsilon\ ^{37}Cl = -0.15 \pm 0.1‰$; Figure 4b) implying that also Van der Waals

interactions lead to stronger net vibrations in the liquid phase. When taking hexadecane partitioning as proxy for non-directed association with organic matter (OM) and combining this isotopic information into a Bordwell thermodynamic cycle[51] the enrichment factor of water/OM partitioning can be calculated, resulting in an insignificant chlorine isotope effect of 0.02‰ ± 0.1‰ (Figure 4c). From these results, we are led to exclude non-specific intermolecular interactions of the chlorine atoms with surrounding cell material as the trigger for inverse chlorine isotope effects in strain UNSWDHB. In contrast, directed interactions of TCM with cellular structures must contribute to the unprecedented inverse isotope effects over and above the contribution made by TmrA. This could involve reversible binding of TCM to docking sites in the periplasmic space, or in channels facilitating substrate transport into the periplasmic space. More investigation is required to uncover the reason(s) for the inverse chlorine isotope effect. An overview of the chlorine and carbon isotope enrichment factors in all investigated systems is presented (Figure 5). The figure highlights the similarity in carbon and chlorine isotope effects of Vitamin B_{12} and strain CF as well as the strong contrast in isotope effects of strain UNSWDHB and these two systems.

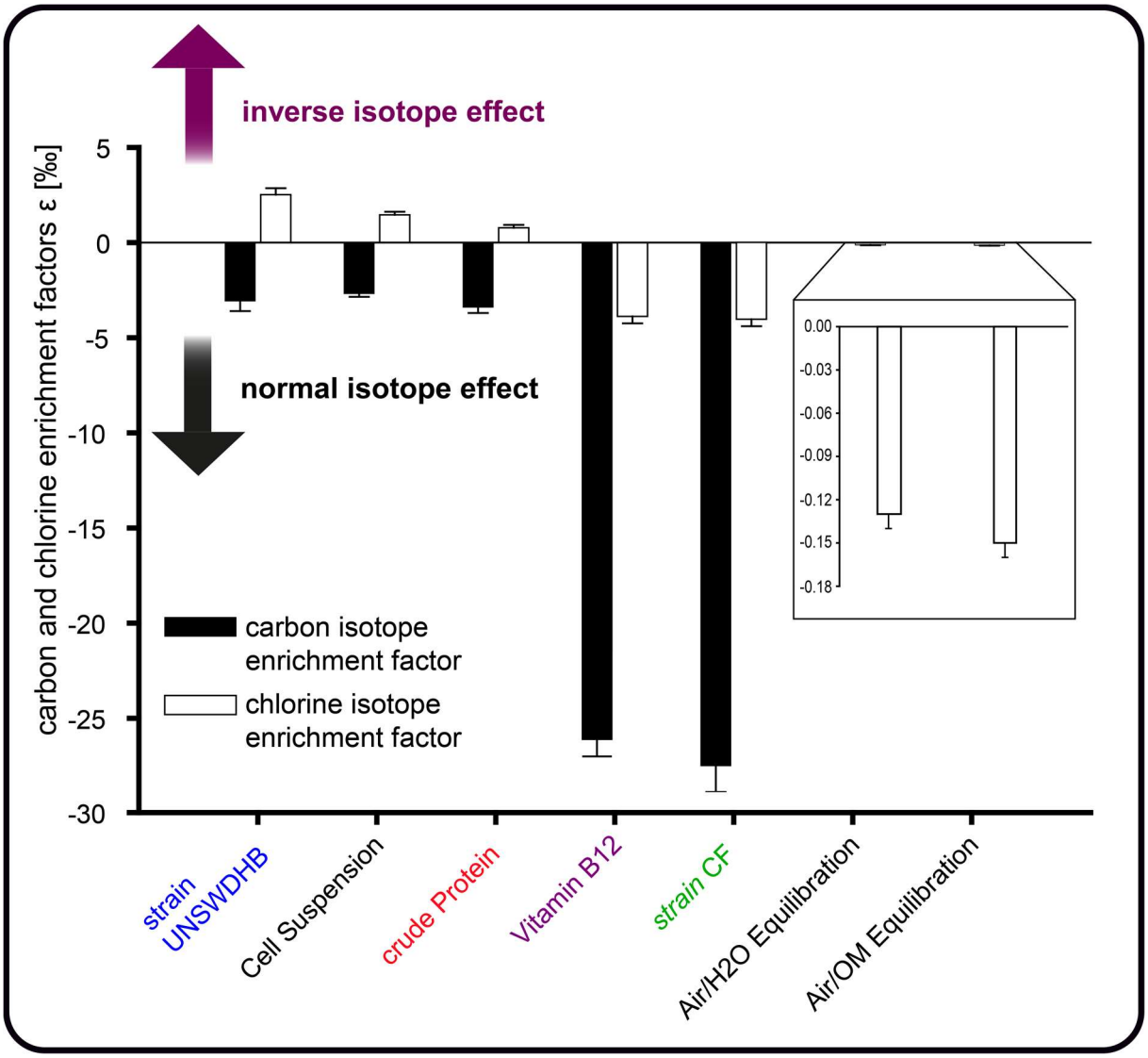

Figure 5: Comparison of the different carbon and chlorine isotopic enrichment factors including: Strain UNSWDHB (bacteria), cell suspensions and protein extracts (protein), VB12 partitioning experiments and the strain CF[8]

Isotope effects suggest either an outer-sphere single electron transfer or a S_N2 reaction mechanism for TCM reduction by Vitamin B_{12} and strain CF

While the enzyme mechanism in strain UNSWDHB remains elusive, the strong isotope fractionation of TCM in transformation by strain CF and with Vitamin B_{12} allows for the exploration of possible underlying reaction mechanisms in these systems. Previous studies have focused on monitoring stable isotope effects in TCM during various dehalogenation reactions (e.g. zero valent iron, persulfate, alkaline hydrolysis and outer-sphere single electron transfer

513 reactions (OS-SET))[2]. By summarizing the isotope effects from this study and previous results
514 in a dual element isotope plot, the striking similarity of the λ values from TCM reduction by
515 strain CF (λ = 6.6 ± 0.1), Vitamin B_{12} (λ = 6.5 ± 0.2) and the OS-SET model system (λ = 6.7 ±
516 0.4) becomes obvious. While, this provides circumstantial evidence that Vitamin B_{12} and strain
517 CF react via an OS-SET with TCM; the evidence is weakened by two observations. First, when
518 AKIE values are taken into account, differences become apparent. Similar $AKIE_C$ and $AKIE_{Cl}$
519 values are recorded for the reaction of TCM with strain CF ($AKIE_C$ = 1.028 ± 0.0009; $AKIE_{Cl}$
520 = 1.013 ± 0.0002) and Vitamin B_{12} ($AKIE_C$ = 1.026 ± 0.0009; $AKIE_{Cl}$ = 1.012 ± 0.0002), but
521 contrast with smaller AKIE values for the OS-SET reaction ($AKIE_C$ = 1.018 ± 0.0008; $AKIE_{Cl}$
522 = 1.008 ± 0.0002). Second, the OS-SET transfer reaction would not be able to explain the
523 product formation in the case of Vitamin B_{12}. Simultaneous formation of DCM, chloromethane
524 and methane during the reductive dehalogenation of TCM by Vitamin B_{12} (Figure 2) indicate
525 parallel product formation. This observation is supported by the carbon isotope values of DCM
526 and chloromethane. Here, greater $^{13}C/^{12}C$ ratios are detected for chloromethane compared to
527 DCM (chloromethane $\delta^{13}C$ = -68‰ and DCM $\delta^{13}C$ = -80‰ at f = 0.8, see Figure S2). In a
528 sequential product formation, smaller $^{13}C/^{12}C$ ratios (more negative $\delta^{13}C$ values) would be
529 expected for chloromethane, as it would have to be formed as a product of DCM. Therefore, in
530 the case of parallel product formation chloromethane has to be formed directly from TCM.
531 This, however, would not be possible with radicals in solution, but would require stabilization
532 of intermediates. Such a more intimate reaction chemistry could be initiated by a S_N2 reaction
533 mechanism where organometallic intermediates are formed. Based on these contradictions,
534 further investigation is necessary to resolve whether an OS-SET or S_N2 reaction mechanism is
535 responsible for TCM dehalogenation with Vitamin B_{12} and strain CF.

536 In summary, the overall TCM dehalogenation isotope values provided by strain UNSWDHB
537 contrast strongly with other abiotic and biotic TCM degradation systems (Figure 6). Such a
538 contrast suggests that dual isotope CSIA could be a useful technique for determining *in situ*

activity of strain UNSWDHB, particularly if complemented with molecular techniques that target functional and phylogenetic markers genes (i.e. qPCR with 16S rNRA and *tmr*A specific primers).

542 **Table 1:** AKIE values, isotopic enrichment factors and values from dual element isotope slopes from biotic and abiotic TCM degradation provided

543 from this study and previous studies

Experiment with TCM	Possible reaction mechanism	$AKIE_C$	$AKIE_{Cl}$	ε_C [‰]	ε_{Cl} [‰]	λ	published
Strain UNSWDHB	masked	1.003 ± 0.0005	0.997 ± 0.0003	-3.1 ± 0.5	2.5 ± 0.3	-1.2 ± 0.2	This study
Strain CF	S_N2 or OS -SET	1.028 ± 0.0009	1.013 ± 0.0002	-27.9 ± 1.7	-4.2 ± 0.2	6.6 ± 0.1	This study
Vitamin B12	S_N2 or OS -SET	1.026 ± 0.0009	1.012 ± 0.0002	-26.0 ± 0.9	-4.0 ± 0.2	6.5 ± 0.2	This study
CO_2 radical anions (OS-SET)	OS -SET	1.018 ± 0.0008	1.008 ± 0.0002	-17.7 ± 0.8	-2.6 ± 0.2	6.7 ±0 .4	Heckel et al.[21]
Zero valent iron		1.034 ± 0.012	1.008 ± 0.001	-33 ± 11	-3 ± 1	8 ± 2	Torrento et al.[2]
Alkaline hydrolysis	$E1_{CB}$ elimination	1.061 ± 0.006	1.0133 ± 0.0004	-57 ± 5	-4.4 ± 0.4	13.0 ± 0.8	Torrento et al.[2]
Persulfate oxidation	Oxidative C-H bond cleavage	1.008 ± 0.001	1.00045 ± 0.00004	-8 ± 1	-0.44 ± 0.06	17 ± 2	Torrento et al.[2]

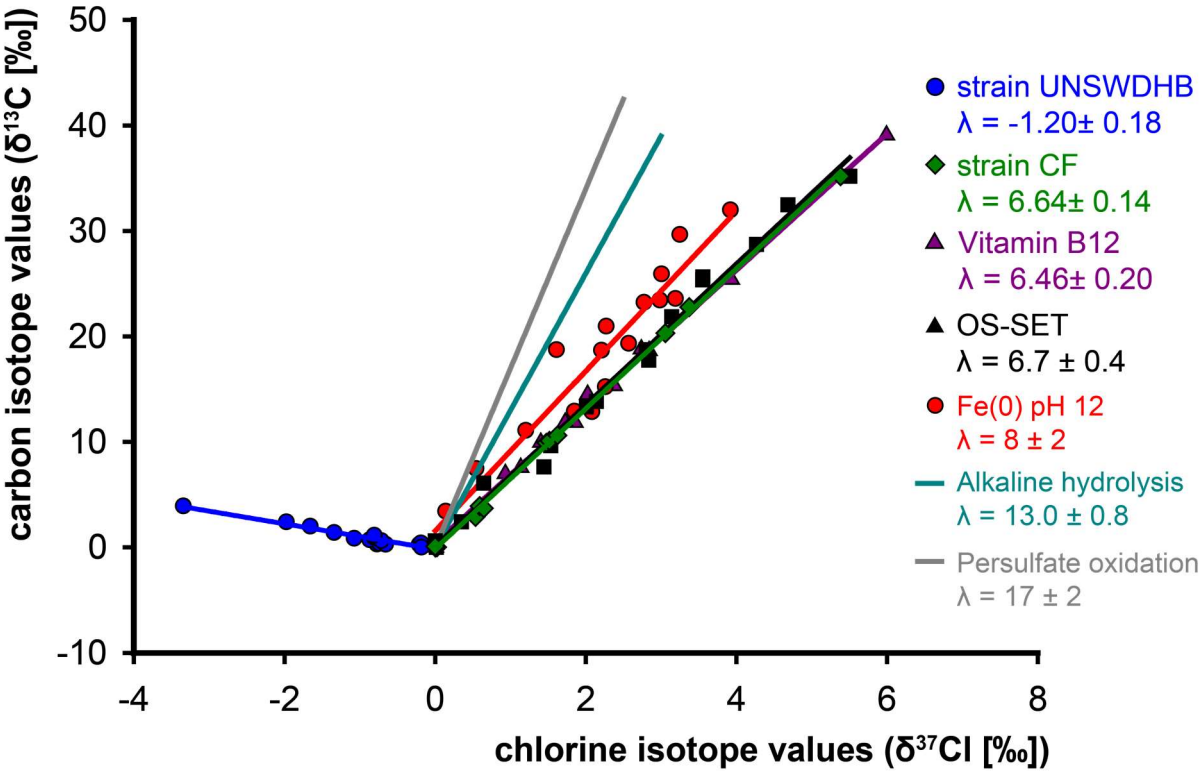

Figure 6: Comparison of the dual element isotope slopes of TCM transformation by strains UNSWDHB and CF and Vitamin B_{12} with slopes of TCM transformations by alkaline hydrolysis, persulfate oxidation, zero valent iron, and with outer sphere single electron transfer (OS-SET)[2, 26].

ENVIRONMENTAL SIGNIFICANCE

Uncovering degradation processes or reaction mechanisms in complex natural transformations is intrinsically difficult. A first necessary step to understand these processes is an understanding of degradation pathways to problematic or harmless products (e.g. DCM vs. CH_4). Multi-element isotope effect analysis of organic compounds at natural isotopic abundance provides the possibility to pinpoint such processes or chemical reactions[21, 44, 52, 53]. Concerning the identification of reaction mechanisms, there are also limitations with compound specific isotope analysis e.g. masking of the intrinsic isotope effect, which has been demonstrated here with

559 TCM and also in previous studies with PCE[19, 20, 54]. By comparing the isotope effects of TCM
560 reductive dechlorination strain UNSWDHB with strain CF, we were able to reveal pronounced
561 carbon and chlorine isotope effects with strain CF and masked and inverse chlorine isotope
562 effects with strain UNSWDHB. Experiments with crude protein extract, cell suspension and
563 respiring cells, furthermore, illustrated that the inverse chlorine isotope effect increased with
564 increasing complexity of the systems. Additionally, we were able to gain strong evidence that
565 strain CF and the enzymatic cofactor Vitamin B_{12} share a common reaction mechanism,
566 possibly either OS-SET or S_N2.

567 In the end, we obtained evidence that the dual element isotope slope of TCM reduction by strain
568 CF reflects the reaction with the enzymatic cofactor within the RDase, whereas in the case of
569 UNSWDHB it reflects the RDase kinetics in which the coenzyme reaction is masked plus
570 additional contributions from directed interactions prior to catalysis. We observed furthermore
571 that the reductive dehalogenation of TCM by vitamin B_{12} resulted in parallel product formation
572 (DCM, chloromethane and methane) in contrast to the single product formation by strain CF
573 and UNSWDHB. This leaves the question why a possibly identical reaction mechanism leads
574 to different product formation? Further mechanistic investigations might answer the question
575 of how TCM is degraded, but not necessarily why the reaction stops at DCM. The uptake of the
576 substrate by the enzyme pocket and especially the enzyme 3D structure might help answer why
577 the reaction stalls at DCM in case of strains CF and UNSWDHB. Therefore, investigations
578 concerning the RDase structure could be the key to solving this question and also to uncovering
579 the differences of the enzymatic reaction of strain CF and UNSWDHB. Ultimately, such an in-
580 depth mechanistic understanding may point the way to possible solutions for faster and
581 complete dehalogenation of harmful halogenated methanes.

582

583 ASSOCIATED CONTENT

584 **Supporting Information**

585 The Supporting Information is available free of charge on the ACS Publications website.

586 Consisting of additional figures which were mentioned in the manuscript

587

588 AUTHOR INFORMATION

589 **Corresponding Authors**

590 *Phone: +49 89 3187 3736; e-mail: benjamin.heckel@tum.de

591 & Phone: + 61 02 9385 5017; e-mail: mattlee@unsw.edu.au

592 **Author Contributions**

593 The manuscript was written through contributions of all authors. All authors have given

594 approval to the final version of the manuscript.

595 **Notes**

596 The authors declare no competing financial interest.

597

598 ACKNOWLEDGMENT

599 This work was supported by Helmholtz Zentrum München of the Helmholtz Association of

600 German research centers, by the German Research Foundation (DFG), EL 266/3-1/2 and

601 Natural Sciences and Engineering Council of Canada (NSERC).

602

603 ## References

604

605 1. Hunkeler, D.; Laier, T.; Breider, F.; Jacobsen, O. S., Demonstrating a Natural Origin
606 of Chloroform in Groundwater Using Stable Carbon Isotopes. *Environ. Sci. Technol.* **2012,**
607 *46*, (11), 6096-6101.
608 2. Torrentó, C.; Palau, J.; Rodríguez-Fernández, D.; Heckel, B.; Meyer, A.; Domènech,
609 C.; Rosell, M.; Soler, A.; Elsner, M.; Hunkeler, D., Carbon and Chlorine Isotope
610 Fractionation Patterns Associated with Different Engineered Chloroform Transformation
611 Reactions. *Environ. Sci. Technol.* **2017,** *51*, (11), 6174-6184.

3. U.S. EPA *Assessment of the Potential Impacts of Hydraulic Fracturing for Oil and Gas on Drinking Water Resources*; Washington, DC,, 2015.
4. Jugder, B.-E.; Ertan, H.; Bohl, S.; Lee, M.; Marquis, C. P.; Manefield, M., Organohalide Respiring Bacteria and Reductive Dehalogenases: Key Tools in Organohalide Bioremediation. *Front. Microbiol.* **2016,** *7*, (249).
5. Lee, M.; Wells, E.; Wong, Y. K.; Koenig, J.; Adrian, L.; Richnow, H. H.; Manefield, M., Relative Contributions of Dehalobacter and Zerovalent Iron in the Degradation of Chlorinated Methanes. *Environ. Sci. Technol.* **2015,** *49*, (7), 4481-4489.
6. Lee, P. K. H.; Warnecke, F.; Brodie, E. L.; Macbeth, T. W.; Conrad, M. E.; Andersen, G. L.; Alvarez-Cohen, L., Phylogenetic Microarray Analysis of a Microbial Community Performing Reductive Dechlorination at a TCE-Contaminated Site. *Environ. Sci. Technol.* **2012,** *46*, (2), 1044-1054.
7. Wong, Y. K.; Holland, S. I.; Ertan, H.; Manefield, M.; Lee, M., Isolation and characterization of *Dehalobacter* sp. strain UNSWDHB capable of chloroform and chlorinated ethane respiration. *Environ. Microbiol.* **2016,** *18*, (9), 3092-3105.
8. Chan, C. C. H.; Mundle, S. O. C.; Eckert, T.; Liang, X.; Tang, S.; Lacrampe-Couloume, G.; Edwards, E. A.; Sherwood Lollar, B., Large Carbon Isotope Fractionation during Biodegradation of Chloroform by *Dehalobacter* Cultures. *Environ. Sci. Technol.* **2012,** *46*, (18), 10154-10160.
9. Tang, S.; Chan, W. W.; Fletcher, K. E.; Seifert, J.; Liang, X.; Löffler, F. E.; Edwards, E. A.; Adrian, L., Functional characterization of reductive dehalogenases by using blue native polyacrylamide gel electrophoresis. *Appl. Environ. Microbiol.* **2013,** *79*, (3), 974-981.
10. Deshpande, N. P.; Wong, Y. K.; Manefield, M.; Wilkins, M. R.; Lee, M., Genome Sequence of *Dehalobacter* UNSWDHB, a Chloroform-Dechlorinating Bacterium. *Genome Announc.* **2013,** *1*, (5), e00720-13.
11. Ding, C.; Zhao, S.; He, J., A *Desulfitobacterium* sp. strain PR reductively dechlorinates both 1,1,1‐trichloroethane and chloroform. *Environ. Microbiol.* **2014,** *16*, (11), 3387-3397.
12. Jugder, B.-E.; Ertan, H.; Wong, Y. K.; Braidy, N.; Manefield, M.; Marquis, C. P.; Lee, M., Genomic, transcriptomic and proteomic analyses of *Dehalobacter* UNSWDHB in response to chloroform. *Environ. Microbio.l Rep.* **2016,** *8*, (5), 814-824.
13. Grostern, A.; Duhamel, M.; Dworatzek, S.; Edwards, E. A., Chloroform respiration to dichloromethane by a *Dehalobacter* population. *Environ. Microbiol.* **2010,** *12*, (4), 1053-1060.
14. Kunze, C.; Bommer, M.; Hagen, W. R.; Uksa, M.; Dobbek, H.; Schubert, T.; Diekert, G., Cobamide-mediated enzymatic reductive dehalogenation via long-range electron transfer. *Nat. Commun.* **2017,** *8*, 15858.
15. Bommer, M.; Kunze, C.; Fesseler, J.; Schubert, T.; Diekert, G.; Dobbek, H., Structural basis for organohalide respiration. *Science* **2014,** *346*, (6208), 455-458.
16. Abe, Y.; Aravena, R.; Zopfi, J.; Shouakar-Stash, O.; Cox, E.; Roberts, J. D.; Hunkeler, D., Carbon and Chlorine Isotope Fractionation during Aerobic Oxidation and Reductive Dechlorination of Vinyl Chloride and cis-1,2-Dichloroethene. *Environ. Sci. Technol.* **2009,** *43*, (1), 101-107.
17. Audí-Miró, C.; Cretnik, S.; Otero, N.; Palau, J.; Shouakar-Stash, O.; Soler, A.; Elsner, M., Cl and C isotope analysis to assess the effectiveness of chlorinated ethene degradation by zero-valent iron: Evidence from dual element and product isotope values. *Appl. Geochem.* **2013,** *32*, (0), 175-183.
18. Cretnik, S.; Thoreson, K. A.; Bernstein, A.; Ebert, K.; Buchner, D.; Laskov, C.; Haderlein, S.; Shouakar-Stash, O.; Kliegman, S.; McNeill, K.; Elsner, M., Reductive Dechlorination of TCE by Chemical Model Systems in Comparison to Dehalogenating

662 Bacteria: Insights from Dual Element Isotope Analysis (13C/12C, 37Cl/35Cl). *Environ. Sci.*
663 *Technol.* **2013,** *47*, (13), 6855-6863.
664 19. Wiegert, C.; Mandalakis, M.; Knowles, T.; Polymenakou, P. N.; Aeppli, C.;
665 Macháčková, J.; Holmstrand, H.; Evershed, R. P.; Pancost, R. D.; Gustafsson, Ö., Carbon and
666 Chlorine Isotope Fractionation During Microbial Degradation of Tetra- and Trichloroethene.
667 *Environ. Sci. Technol.* **2013,** *47*, (12), 6449-6456.
668 20. Renpenning, J.; Keller, S.; Cretnik, S.; Shouakar-Stash, O.; Elsner, M.; Schubert, T.;
669 Nijenhuis, I., Combined C and Cl Isotope Effects Indicate Differences between Corrinoids
670 and Enzyme (*Sulfurospirillum multivorans* PceA) in Reductive Dehalogenation of
671 Tetrachloroethene, But Not Trichloroethene. *Environ. Sci. Technol.* **2014,** *48*, (20), 11837–
672 11845.
673 21. Heckel, B.; Cretnik, S.; Kliegman, S.; Shouakar-Stash, O.; McNeill, K.; Elsner, M.,
674 Reductive Outer-Sphere Single Electron Transfer Is an Exception Rather than the Rule in
675 Natural and Engineered Chlorinated Ethene Dehalogenation. *Environ. Sci. Technol.* **2017,** *51*,
676 (17), 9663-9673.
677 22. Hoefs, J., *Stable Isotope Geochemistry*. Springer-Verlag: Berlin, 1997.
678 23. Elsner, M.; Zwank, L.; Hunkeler, D.; Schwarzenbach, R. P., A new concept linking
679 observable stable isotope fractionation to transformation pathways of organic pollutants.
680 *Environ. Sci. Technol.* **2005,** *39*, (18), 6896-6916.
681 24. Meyer, A. H.; Penning, H.; Elsner, M., C and N isotope fractionation suggests similar
682 mechanisms of microbial atrazine transformation despite involvement of different Enzymes
683 (AtzA and TrzN). *Environ. Sci. Technol.* **2009,** *43*, (21), 8079-8085.
684 25. Kuder, T.; van Breukelen, B. M.; Vanderford, M.; Philp, P., 3D-CSIA: Carbon,
685 Chlorine, and Hydrogen Isotope Fractionation in Transformation of TCE to Ethene by a
686 *Dehalococcoides* Culture. *Environ. Sci. Technol.* **2013,** *47*, (17), 9668-9677.
687 26. Heckel, B.; Rodríguez-Fernández, D.; Torrentó, C.; Meyer, A.; Palau, J.; Domènech,
688 C.; Rosell, M.; Soler, A.; Hunkeler, D.; Elsner, M., Compound-Specific Chlorine Isotope
689 Analysis of Tetrachloromethane and Trichloromethane by Gas Chromatography-Isotope Ratio
690 Mass Spectrometry vs Gas Chromatography-Quadrupole Mass Spectrometry: Method
691 Development and Evaluation of Precision and Trueness. *Anal. Chem.* **2017,** *89*, (6), 3411-
692 3420.
693 27. Elsner, M., Stable isotope fractionation to investigate natural transformation
694 mechanisms of organic contaminants: principles, prospects and limitations. *J. Environ. Monit.*
695 **2010,** *12*, (11), 2005-2031.
696 28. Hofstetter, T. B.; Berg, M., Assessing transformation processes of organic
697 contaminants by compound-specific stable isotope analysis. *TrAC, Trends Anal. Chem.* **2011,**
698 *30*, (4), 618-627.
699 29. Vogt, C.; Dorer, C.; Musat, F.; Richnow, H.-H., Multi-element isotope fractionation
700 concepts to characterize the biodegradation of hydrocarbons — from enzymes to the
701 environment. *Curr. Opin. Biotechnol.* **2016,** *41*, 90-98.
702 30. Heckel, B.; McNeill, K.; Elsner, M., Chlorinated Ethene Reactivity with Vitamin B12
703 Is Governed by Cobalamin Chloroethylcarbanions as Crossroads of Competing Pathways.
704 *ACS Catal.* **2018,** *8*, (4), 3054-3066.
705 31. Palau, J.; Jamin, P.; Badin, A.; Vanhecke, N.; Haerens, B.; Brouyère, S.; Hunkeler, D.,
706 Use of dual carbon–chlorine isotope analysis to assess the degradation pathways of 1,1,1-
707 trichloroethane in groundwater. *Water Res.* **2016,** *92*, 235-243.
708 32. Northrop, D. B., The expression of isotope effects on enzyme-catalyzed reactions.
709 *Annu. Rev. Biochem.* **1981,** *50*, 103-131.
710 33. Nijenhuis, I.; Andert, J.; Beck, K.; Kastner, M.; Diekert, G.; Richnow, H. H., Stable
711 isotope fractionation of tetrachloroethene during reductive dechlorination by *Sulfurospirillum*

multivorans and *Desulfitobacterium* sp. Strain PCE-S and abiotic reactions with cyanocobalamin. *Appl. Environ. Microbiol.* **2005,** *71*, (7), 3413-3419.
34. Edwards, E. A.; Grbić-Galić, D., Anaerobic degradation of toluene and o-xylene by a methanogenic consortium. *Appl. Environ. Microbiol.* **1994,** *60*, (1), 313-322.
35. Bernstein, A.; Shouakar-Stash, O.; Ebert, K.; Laskov, C.; Hunkeler, D.; Jeannottat, S.; Sakaguchi-Söder, K.; Laaks, J.; Jochmann, M. A.; Cretnik, S.; Jager, J.; Haderlein, S. B.; Schmidt, T. C.; Aravena, R.; Elsner, M., Compound-Specific Chlorine Isotope Analysis: A Comparison of Gas Chromatography/Isotope Ratio Mass Spectrometry and Gas Chromatography/Quadrupole Mass Spectrometry Methods in an Interlaboratory Study. *Anal. Chem.* **2011,** *83*, (20), 7624-7634.
36. Schwarzenbach, R. P.; Gschwend, P. M.; Imboden, D. M., *Environmental Organic Chemistry*. second edition ed.; John Wiley & Sons, Inc.: New Jersey, 2003; p 1313.
37. Holliger, C.; Wohlfarth, G.; Diekert, G., Reductive dechlorination in the energy metabolism of anaerobic bacteria. *FEMS Microbiol Rev* **1998,** *22*, (5), 383-398.
38. Neumann, A.; Scholz-Muramatsu, H.; Diekert, G., Tetrachloroethene metabolism of *Dehalospirillum multivorans*. *Arch. Microbio.l* **1994,** *162*, (4), 295-301.
39. Torgonskaya, M. L.; Zyakun, A. M.; Trotsenko, Y. A.; Laurinavichius, K. S.; Kümmel, S.; Vuilleumier, S.; Richnow, H. H., Individual stages of bacterial dichloromethane degradation mapped by carbon and chlorine stable isotope analysis. *J. Environ. Sci.* **2018**.
40. Sherwood Lollar, B.; Hirschorn, S.; Mundle, S. O. C.; Grostern, A.; Edwards, E. A.; Lacrampe-Couloume, G., Insights into Enzyme Kinetics of Chloroethane Biodegradation Using Compound Specific Stable Isotopes. *Environ. Sci. Technol.* **2010,** *44*, (19), 7498-7503.
41. Jugder, B. E.; Bohl, S.; Lebhar, H.; Healey, R. D.; Manefield, M.; Marquis, C. P.; Lee, M., A bacterial chloroform reductive dehalogenase: purification and biochemical characterization. *Trends Biotechnol.* **2017,** *10*, (6), 1640-1648.
42. Aeppli, C.; Berg, M.; Cirpka, O. A.; Holliger, C.; Schwarzenbach, R. P.; Hofstetter, T. B., Influence of Mass-Transfer Limitations on Carbon Isotope Fractionation during Microbial Dechlorination of Trichloroethene. *Environ. Sci. Technol.* **2009,** *43*, (23), 8813-8820.
43. Jin, B.; Rolle, M.; Li, T.; Haderlein, S. B., Diffusive Fractionation of BTEX and Chlorinated Ethenes in Aqueous Solution: Quantification of Spatial Isotope Gradients. *Environ. Sci. Technol.* **2014,** *48*, (11), 6141-6150.
44. Heckel, B.; McNeill, K.; Elsner, M., Chlorinated Ethene Reactivity with Vitamin B12 Is Governed by Cobalamin Chloroethylcarbanions as Crossroads of Competing Pathways. *ACS Catalysis* **2018**.
45. Melander, L.; Saunders, W. H., *Reaction rates of isotopic molecules*. John Wiley: New York, 1980; p 331.
46. Marlier, J. F., Multiple isotope effects on the acyl group transfer reactions of amides and esters. *Acc. Chem. Res.* **2001,** *34*, (4), 283-290.
47. Horst, A.; Lacrampe-Couloume, G.; Sherwood Lollar, B., Vapor Pressure Isotope Effects in Halogenated Organic Compounds and Alcohols Dissolved in Water. *Anal. Chem.* **2016,** *88*, (24), 12066-12071.
48. Kopinke, F.-D.; Georgi, A., Comment on Vapor Pressure Isotope Effects in Halogenated Organic Compounds and Alcohols Dissolved in Water. *Anal. Chem.* **2017,** *89*, (19), 10637-10638.
49. Jancsó, G.; Van Hook, W. A., Condensed phase isotope effects (especially vapor pressure isotope effects). *Chem. Rev.* **1974,** *74*, 689-750.
50. Jancso, G.; Rebelo, L. P. N.; Vanhook, W. A., Isotope Effects in Solution Thermodynamics - Excess Properties in Solutions of Isotopomers. *Chem. Rev.* **1993,** *93*, (8), 2645-2666.
51. Bordwell, F. G., Equilibrium acidities in dimethyl sulfoxide solution. *Acc. Chem. Res.* **1988,** *21*, (12), 456-463.

763 52. Palau, J.; Cretnik, S.; Shouakar-Stash, O.; Höche, M.; Elsner, M.; Hunkeler, D., C and
764 Cl Isotope Fractionation of 1,2-Dichloroethane Displays Unique δ13C/δ37Cl Patterns for
765 Pathway Identification and Reveals Surprising C–Cl Bond Involvement in Microbial
766 Oxidation. *Environ. Sci. Technol.* **2014,** *48*, (16), 9430-9437.
767 53. Palau, J.; Shouakar-Stash, O.; Hatijah Mortan, S.; Yu, R.; Rosell, M.; Marco-Urrea,
768 E.; Freedman, D. L.; Aravena, R.; Soler, A.; Hunkeler, D., Hydrogen Isotope Fractionation
769 during the Biodegradation of 1,2-Dichloroethane: Potential for Pathway Identification Using a
770 Multi-element (C, Cl, and H) Isotope Approach. *Environ. Sci. Technol.* **2017,** *51*, (18), 10526-
771 10535.
772 54. Badin, A.; Buttet, G.; Maillard, J.; Holliger, C.; Hunkeler, D., Multiple Dual C–Cl
773 Isotope Patterns Associated with Reductive Dechlorination of Tetrachloroethene. *Environ.*
774 *Sci. Technol.* **2014,** *48*, (16), 9179-9186.

775